Collective Excitations in Antidots

K. Kern, D. Heitmann, P. Grambow, Y. H. Zhang, and K. Ploog
Max-Planck-Institut für Festkörperforschung, Heisenbergstrasse 1, D-7000 Stuttgart 80, Federal Republic of Germany
(Received 19 October 1990)

Antidot structures have been prepared by etching arrays of 100-nm holes into a two-dimensional electron gas of $Ga_xIn_{1-x}As$ quantum wells. In the far-infrared response we observe the unique collective excitation spectrum of antidots. It consists of a high-frequency branch which starts, in a magnetic field B, with a negative B dispersion and then increases in frequency with B. A second low-frequency branch corresponds at high B to edge magnetoplasmons which circulate around the holes. For small B this branch approaches the cyclotron frequency, where the electrons perform classical cyclotron orbits around the holes.

PACS numbers: 72.15.Rn, 73.20.Dx, 73.20.Mf

With today's highly sophisticated submicron lithography it has become possible to prepare very small lateral structures starting from two-dimensional electron systems (2DES) in semiconductors. The ultimate limits are quantum dots, artificial "atoms" which contain only a very small number of electrons on discrete energy levels.[1-7] A reversed structure with respect to dots is "antidots," where "holes" are "punched" into a 2DES. There are already several investigations on the transport properties of antidots,[8,9] in particular in search for incommensurability phenomena and the Hofstädter butterfly in magnetic fields. We have investigated the far-infrared (FIR) excitation spectrum in perpendicular magnetic fields B and observed unique collective excitations which, to our knowledge, have so far not been observed or theoretically predicted. In particular, we observe two branches. A high-frequency resonance exhibits a negative B dispersion at small magnetic fields B and then increases in frequency with B. A second branch at lower frequency corresponds at high B to an edge magnetoplasmon mode which circulates around the circumference of the hole. This low-frequency branch approaches the cyclotron resonance (CR) frequency ω_c at small B where the classical cyclotron orbit is comparable to the hole radius. This indicates that the electrons perform a classical cyclotron orbit around the holes. Exchange of oscillator strength indicates a coupling between the two modes.

Antidot samples have been prepared by deep-mesa etching[10,11] starting from 2DES in modulation-doped $Ga_xIn_{1-x}As/Al_yIn_{1-y}As$ single quantum wells. All samples were grown lattice matched ($x=0.48$, $y=0.47$) on semi-isolating InP substrates by molecular-beam epitaxy. Typical growth sequences and conditions are discussed in Refs. 11 and 12. A photoresist grid mask was prepared by a holographic double exposure and arrays of holes with typical diameters $2r_g=100$–300 nm, were etched 100 nm deep, i.e., through the active layer, into the buffer. The period in both lateral directions was $a=300$–400 nm. A scanning electron micrograph of the antidot structure of sample (b) is shown in Fig. 1(a). The $Ga_xIn_{1-x}As$ system has the advantage of a small effective mass ($m^* \approx 0.042m_0$ at the band edge and $x=0.47$) and, as we have shown in Ref. 11, a very small lateral edge depletion width w_{depl} (estimated <30 nm) at the etched sidewalls of the holes. Thus the "electronic" radius $r_e=r_g+w_{\text{depl}}$ of the hole is not much larger

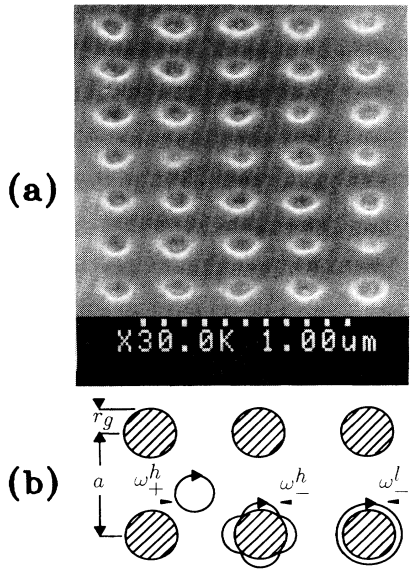

FIG. 1. (a) Scanning electron micrograph taken at an angle of 45° from an antidot array [sample (b)] with a period $a=300$ nm and holes of diameter $2r_g=100$ nm etched into a $Ga_xIn_{1-x}As/Al_yIn_{1-y}As$ single quantum well. (b) Sketch of the antidot structure. Hatched areas are holes punched into a 2DES. The motion of individual electrons is shown schematically for the high-frequency mode (ω_+^h) at high magnetic fields, and for the low-frequency mode at low (ω_-^l) and at high magnetic field (ω_-^h).

than the etched geometrical radius r_g. The two-dimensional charge density N_s in the samples was varied via the persistent photoeffect and was determined *in situ* from Shubnikov-de Haas oscillations in quasi-dc microwave transmission.[11] We will see later that the small effective mass, the small values of r_g, and also the relatively high values of N_s which can be realized in the $Ga_xIn_{1-x}As$ system shift the important features of the antidot excitation spectrum to high frequencies which makes them easier to observe as compared, e.g., to the AlGaAs/GaAs system. FIR transmission experiments have been performed in a superconducting magnet cryostat which was connected to a Fourier-transform spectrometer. The spectral resolution was set to 0.5 cm^{-1}. The temperature was 2.2 K.

Experimental transmission spectra of unpolarized FIR radiation in perpendicular magnetic fields B for the antidot sample (a) with period $a=300$ nm, hole diameter $2r_g=200$ nm, and carrier density $N_s=8\times10^{11}$ cm^{-2} are shown in Fig. 2. We have found that the spectra do not depend on the polarization direction of linearly polarized radiation. Several resonances with different B dispersions are observed. The dispersions and the amplitudes of the resonances are plotted in Fig. 3. The excitation spectrum consists mainly of two modes, a high- and a low-frequency branch labeled ω_+ and ω_-, respectively. The high-frequency resonances ω_+ start for $B=0$ at $\omega_{+0}=94$ cm^{-1}. They first decrease in frequency and then increase with B, approaching at high B the CR frequency ω_c of the 2D sample. The low-frequency branch ω_- starts at small B at $\approx\omega_c$. It then bends down and exhibits for higher B values a negative B dispersion. Figure 3(c) demonstrates that with increasing B, oscillator strength is transferred from the ω_- branch, which has a large amplitude at small B, to the ω_+ branch, which increases in intensity with B. A very similar behavior has been observed on several antidot samples which have been prepared starting from heterostructures and symmetrically or asymmetrically modulation-doped quantum wells with different spacer layers. In Fig. 3(b) we show the dispersion of sample (b) which has an antidot lattice with the same period $a=300$ nm but holes with a smaller diameter of only $2r_g=100$ nm [see Fig. 1(a)] and a

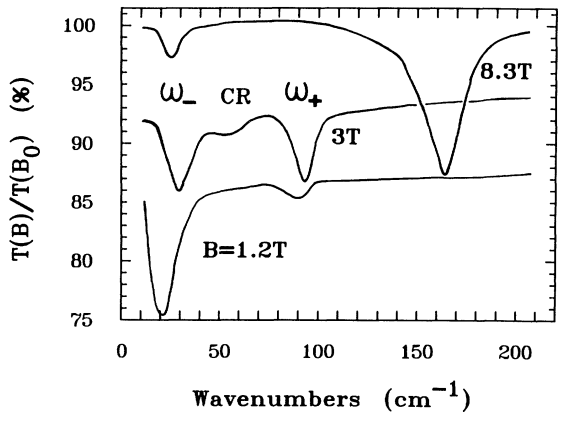

FIG. 2. Normalized transmission spectra of unpolarized FIR radiation through the antidot sample (a) with hole diameter $2r_g=200$ nm and period $a=300$ nm at various magnetic fields B.

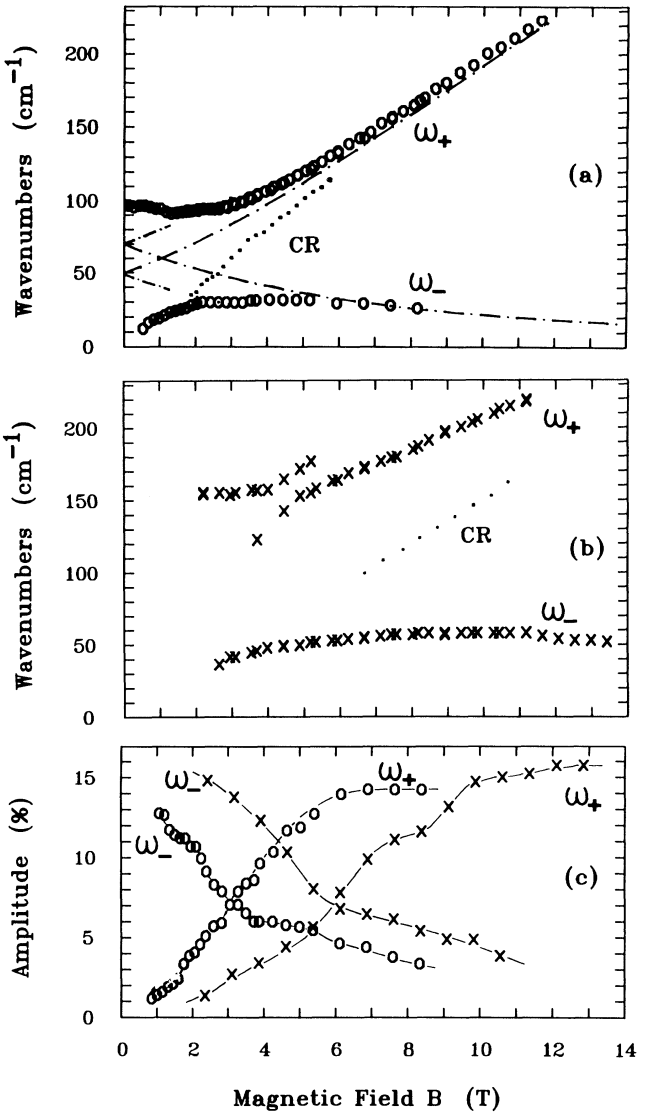

FIG. 3. (a),(b) Experimental dispersions of the high-frequency (ω_+) and the low-frequency branch (ω_-) in the antidot system of sample (a) ($a=300$ nm, $2r_g=200$ nm) and sample (b) ($a=300$ nm, $2r_g=100$ nm), respectively. CR labels the weak resonances near the CR position. Dashed-dotted lines in (a) are the calculated dispersions for dot structures [Eq. (1)] with different ω_0 which have been fitted to either the high- or the low-frequency modes at high B. (c) Amplitude of the antidot excitation for sample (a) (×) and for sample (b) (○).

higher density of $N_s = 2.5 \times 10^{12}$ cm^{-2}. The frequencies of both branches are increased significantly ($\omega_{+0} = 150$ cm^{-1}) and the maximum frequency (55 cm^{-1}) of the ω_- mode is shifted to a higher B value ($B_-^{\max} \approx 8$–9 T) as compared to Fig. 3(a).

This unique excitation spectrum of antidots has so far not been observed or theoretically predicted. We interpret our observations in the following way. At high B the dispersion of both branches resembles the excitation spectrum of quantum dots.[3–7,13,14] For the excitation spectrum of a dot, using the model of a 2D disk with radius r and density N_s, the resonance frequencies are given according to Fetter[14] by

$$\omega_\pm = [\omega_0^2 + (\omega_c/2)^2]^{1/2} \pm \omega_c/2 ,$$
$$\omega_0^2 = N_s e^2/2m^* \epsilon_{\text{eff}} r , \tag{1}$$

where ϵ_{eff} is the effective dielectric function of the surrounding medium. At $B=0$ dots have only one resonance peak at ω_0 which splits with increasing B into two modes. The resonances of the higher branch increase in frequency with B and approach ω_c. The resonances of the lower branch decrease in frequency with increasing B and represent at high B an edge magnetoplasmon mode, i.e., a collective mode where the individual electrons perform skipping orbits along the circumference inside the dot. For antidots the individual electrons perform skipping orbits along the circumference outside the hole. We have sketched these orbits for high B, ω_-^h, in Fig. 1(b). For high B there is not much difference between a dot or an antidot system since here the edge magnetoplasmon frequency is only governed by the circumference of the structure. Thus, also for antidots, we find that with decreasing B the resonances of the low-frequency branch ω_- first increase in frequency. But then, in contrast to dots, starting at a certain magnetic field $B_-^{\max}$, the resonances in antidots *decrease* in frequency and approach ω_c. This means that the orbits of the ω_- mode become larger and eventually the electrons can perform classical cyclotron orbits $r_c = (2\pi N_s)^{1/2}\hbar/eB$ around the hole. Thus the collective edge-magnetoplasmon excitation gradually changes into a classical CR-like excitation.

We have estimated the value $B_c = (2\pi N_s)^{1/2}\hbar/er_g$ where the classical cyclotron radius r_c becomes equal to the radius of the holes r_g and find for the sample (a) shown in Fig. 3(a) $B_c = 1.4$ T (or, including 25-nm depletion width, $B_c = 1$ T). This is indeed the regime where the resonance frequency is close to ω_c and the edge magnetoplasmon mode has changed to a classical CR motion around the hole. For sample (b) with the smaller hole diameter $2r_g = 100$ nm and the larger N_s we have a larger value of $B_c = 5$ T (3.3 T including 25-nm edge depletion). Indeed, we observe in Fig. 3(b) that the resonances of the ω_- branch are shifted to higher frequencies as compared to Fig. 3(a) and at $B = 3$ T the ω_- mode is very close to the CR. We can observe this upward shift of B_c and $B_-^{\max}$ also directly on one and the same sample if we increase N_s via the persistent photoeffect. This strongly supports our interpretation.

The high-frequency mode which increases in intensity with increasing B represents at small B a plasmon type of collective excitation of all electrons. A unique behavior is that at small B this resonance shows a weak, but distinct, negative B dispersion which was observed on all our samples where we were able to evaluate the resonance position down to $B \approx 0$. In dots, a positive B dispersion is found,[3–7] and confined local plasmon oscillations in wire structures start without and then exhibit a positive B dispersion (e.g., Ref. 10). Another interesting feature as shown in Fig. 3(c) is that with increasing B the oscillator strength is transferred from the ω_- to the ω_+ mode, which clearly indicates a coupling between the two modes.

At higher fields the ω_+ branch approaches ω_c and represents, as denoted in Fig. 1(b) by ω_+^h, a CR type of excitation in the region between the holes. This is supported by the observation that we find different values of ω_0 for the ω_+ (48 cm^{-1}) and the ω_- branch (68 cm^{-1}) if we fit the high-B regime with the dot dispersion (1). This reflects the fact that the confining diameter is, in principle, different for the ω_- and the ω_+ mode. For the ω_- mode it is determined by the hole diameter $2r_g$ [200 nm for sample (a), 100 nm for sample (b)], and for the ω_+ mode approximately by a diameter between four neighboring holes (220 and 320 nm). Thus we expect different values for ω_0.

Within the remaining space we can only briefly discuss several further important findings. On all our samples we observe, weakly as compared to the ω_- mode (see the 3 T curve in Fig. 2), a resonance at the position of the CR in the large gap between the ω_- and the ω_+ mode [see Figs. 3(a) and 3(b)]. The intensity of this mode is larger on samples with larger 2DES regions with respect to hole regions. So we believe that the CR mode is an intrinsic feature of the mode spectrum of antidots. Another noteworthy experimental fact is that we observe, especially pronounced on sample (b) in Fig. 3(b), an anticrossing of the ω_+ branch with $2\omega_c$, the harmonic of the CR. We attribute this resonant interaction as arising from nonlocal interaction, i.e., from the Fermi pressure, since it is very similar in strength (which is deduced from the amount of the resonance splitting) to that observed for 2D magnetoplasmons in homogeneous 2DES.[15] It is interesting to note that such nonlocal effects have so far not been observed in isolated quantum wires (e.g., Refs. 10 and 11) and that nonlocal interaction occurs in a very different form, i.e., as a resonant coupling of different magnetoplasmon modes and *not* at $2\omega_c$, in dot structures.[5] We so far do not know whether nonlocal effects are also the origin of the slight oscillations of the ω_+ resonances which we observe for increasing B near the origin [see Fig. 3(a)]. It is also tempting

to speculate that this arises from incommensurability effects between the classical CR orbit and the geometry of the antidot array.[9] However, this interpretation needs further confirmation.

In conclusion, we have investigated the excitation spectrum of antidots. It consists of two branches where the high-frequency branch starts at small B as a collective plasmon excitation with, surprisingly, a negative B dispersion. With increasing B the high-frequency branch approaches the CR. The resonances of the low-frequency branch start at small B as a classical CR excitation with orbits around the holes and approach with increasing B collective edge-magnetoplasmon modes where the individual electrons perform skipping orbits around the circumference of the holes.

We thank E. Vasiliadou and C. Lange for expert help in the etching of the samples and the characterization by scanning electron microscopy. We gratefully acknowledge financial support by the Bundesministerium für Forschung und Technologie.

[1]M. A. Reed, J. N. Randall, R. J. Aggarwal, R. J. Matyi, T. M. Moore, and A. E. Wetsel, Phys. Rev. Lett. **60**, 535 (1988).

[2]W. Hansen, T. P. Smith, III, K. Y. Lee, J. A. Brum, C. M. Knoedler, J. M. Hong, and D. P. Kern, Phys. Rev. Lett. **62**, 2168 (1989).

[3]Ch. Sikorski and U. Merkt, Phys. Rev. Lett. **62**, 2164 (1989).

[4]C. T. Liu, K. Nakamura, D. C. Tsui, K. Ismail, D. A. Antoniadis, and H. I. Smith, Appl. Phys. Lett. **55**, 168 (1989).

[5]T. Demel, D. Heitmann, P. Grambow, and K. Ploog, Phys. Rev. Lett. **64**, 788 (1990).

[6]A. Lorke, J. P. Kotthaus, and K. Ploog, Phys. Rev. Lett. **64**, 2559 (1990).

[7]For a recent review on the FIR response of dots, see U. Merkt, in *Advances in Solid State Physics,* edited by U. Rössler (Vieweg, Braunschweig, 1990), Vol. 30, p. 77.

[8]K. Ensslin and P. M. Petroff, Phys. Rev. B **41**, 12307 (1990).

[9]D. Weiss, K. von Klitzing, and K. Ploog, Surf. Sci. **229**, 88 (1990).

[10]T. Demel, D. Heitmann, P. Grambow, and K. Ploog, Phys. Rev. B **38**, 12732 (1988).

[11]K. Kern, T. Demel, D. Heitmann, P. Grambow, K. Ploog, and M. Razeghi, Surf. Sci. **229**, 256 (1990).

[12]Y. H. Zhang, D. S. Jiang, R. Cingolani, and K. Ploog, Appl. Phys. Lett. **56**, 2195 (1990).

[13]V. Fock, Z. Phys. **47**, 446 (1928).

[14]A. L. Fetter, Phys. Rev. B **32**, 7676 (1985).

[15]E. Batke, D. Heitmann, J. P. Kotthaus, and K. Ploog, Phys. Rev. Lett. **54**, 2367 (1985).

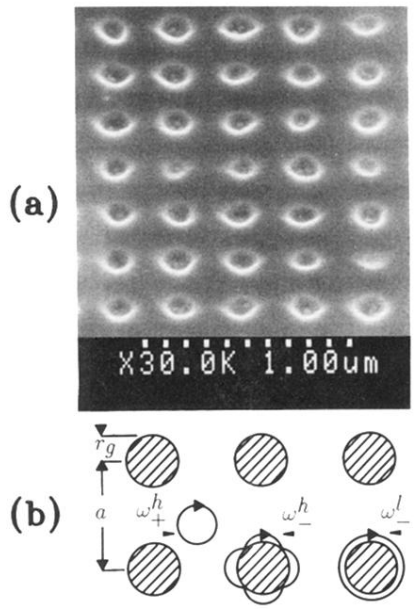

FIG. 1. (a) Scanning electron micrograph taken at an angle of 45° from an antidot array [sample (b)] with a period $a = 300$ nm and holes of diameter $2r_g = 100$ nm etched into a $Ga_xIn_{1-x}As/Al_yIn_{1-y}As$ single quantum well. (b) Sketch of the antidot structure. Hatched areas are holes punched into a 2DES. The motion of individual electrons is shown schematically for the high-frequency mode (ω_+^h) at high magnetic fields, and for the low-frequency mode at low (ω_-^l) and at high magnetic field (ω_-^h).